Evapotranspiration for irrigated agriculture using orbital satellites

Article *in* Bioscience Journal · June 2019

DOI: 10.14393/BJ-v35n3a2019-41737

5 authors, including:

Daniel Althoff
Stockholm University
42 PUBLICATIONS **172** CITATIONS
SEE PROFILE

Francisco Cássio Gomes Alvino
Universidade Federal de Viçosa (UFV)
15 PUBLICATIONS **21** CITATIONS
SEE PROFILE

Roberto Filgueiras
Universidade Federal de Viçosa (UFV)
75 PUBLICATIONS **231** CITATIONS
SEE PROFILE

Catariny Cabral Aleman
Universidade Federal de Viçosa (UFV)
35 PUBLICATIONS **36** CITATIONS
SEE PROFILE

Bioscience Journal Original Article

EVAPOTRANSPIRATION FOR IRRIGATED AGRICULTURE USING ORBITAL SATELLITES

EVAPOTRANSPIRAÇÃO PARA ÁREAS IRRIGADAS UTILIZANDO SATÉLITES ORBITAIS

Daniel ALTHOFF[1]; Francisco Cássio Gomes ALVINO[2]; Roberto FILGUEIRAS[2]; Catariny Cabral ALEMAN[3]; Fernando França da CUNHA[3]

1. MSc student of Agricultural Engineering, Federal University of Viçosa, Viçosa, MG, Brazil. daniel.althoff@ufv.br; 2. PhD student of Agricultural Engineering, Federal University of Viçosa, Viçosa, MG, Brazil; 3. Adjunct Professor, Federal University of Viçosa, Viçosa, MG, Brazil.

ABSTRACT: Acknowledging the importance of evapotranspiration as a mediating factor for efficient irrigation management and water balance, the objective of study is to compare the Simple Algorithm for Evapotranspiration Retrieving (SAFER) to the standard method proposed by FAO-56 for real evapotranspiration, as well as prove its value as an implement in irrigation management for the Brazilian Savanna. Data used refers to 2015's harvest of seven center pivots, located in the municipality of São Desidério in western Bahia. For the SAFER algorithm, the images used were acquired by the Landsat-8 satellite during the entire maize crop cycle. The SAFER algorithm estimation demonstrates the spatial and temporal distribution of the evapotranspiration. A maximum evapotranspiration of 5.38 mm d^{-1} was observed during the crop's reproductive stage. In relation to the standard method, SAFER showed a mean absolute error of 0.40 mm. Thus, concluding that the algorithm can be used to estimate the actual evapotranspiration crop as an alternative to the standard method proposed by FAO-56 for water resources management.

KEYWORDS: Vegetation index. Crop monitoring. Irrigation management. Water balance. Precision irrigation.

INTRODUCTION

The Brazilian savanna biome (Cerrado) is responsible for 70% of the country's agricultural production (THE ECONOMIST, 2010). The success of the Savanna biome in agriculture is due to its favorable climate, which presents rain varying between 500 to 2,000 mm per year (RIBEIRO; WALTER, 1998). However, its precipitation concentrates from October to March, requiring irrigation during the second harvest of the year.

The Cerrado already presents conflicts over different water use in many regions, and the conflicts should rise with the expansion of irrigated areas (MANETA et al., 2009). In order to achieve a rational and efficient management of water use in agriculture, it is important to acquire precise meteorological data to estimate reference evapotranspiration (ET_0). The ET_0 is one of the most important mediating factors for irrigation management, its estimation is based on climatic data of net radiation, temperature, relative humidity of the air and wind speed, consisting of the interaction between energy, weather and hydrology (SANTOS; FONTANA; ALVES, 2011).

The reference evapotranspiration may be obtained by different methods, such as lysimeters, meteorological towers, water balance in the soil or empirical equations such as Penman-Monteith (ALLEN et al., 1998), however, such methodologies present some limitations regarding the estimation values over a specific area. The estimation is rather superficial for an area, not taking in consideration its spatial variation, which is subject to stress from different implying conditions. The acquisition and maintenance of the equipment used for meteorological data observation is also expensive, therefore new methodologies were developed using remote sensing as the main tool (ALLEN et al., 2007; BASTIAANSSEN et al., 1998; TEIXEIRA et al., 2013a; TEIXEIRA et al., 2017). Remote sensing not only allows a rapid data obtainment in a larger scale, but has reduced cost of monitoring (SANTOS; FONTANA; ALVES, 2011).

The remote sensing use is associated to physical and empirical models through algorithms and orbital images. It has been progressively more used to estimate evapotranspiration and to assist on large-scale water resources management in irrigated agriculture (ANDRADE et al., 2014; TEIXEIRA et al., 2015). Among the algorithms that stands out are SEBAL (Surface Energy Balance Algorithm for Land) (BASTIAANSSEN et al., 1998), METRIC (Mapping Evapotranspiration at High Resolution

Received: 16/04/18
Accepted: 05/01/19

with Internalized Calibration) (ALLEN et al., 2007) and SAFER (Simple Algorithm for Evapotranspiration Retrieving) (TEIXEIRA et al., 2013a).

SAFER is, as the name suggests, a simplified algorithm when compared to the others. The theoretical structure and application of the algorithm are associated by means of image processing with the visible, near infrared and thermal infrared bands in conjunction with meteorological data at the time of satellite passage.

The objective of this study was to compare the SAFER algorithm with the standard method (ALLEN et al., 1998) of real evapotranspiration, as well as proves its value as an implement in irrigation management.

MATERIAL AND METHODS

The study area is located in the west of the State of Bahia in the municipality of São Desidério (Figure 1) located in the pair of coordinates 12º27'14" S and 45º41'16" W (*Datum* WGS 84). The region is part of an agricultural frontier (Matopiba), located in the Brazilian Savanna (Cerrado).

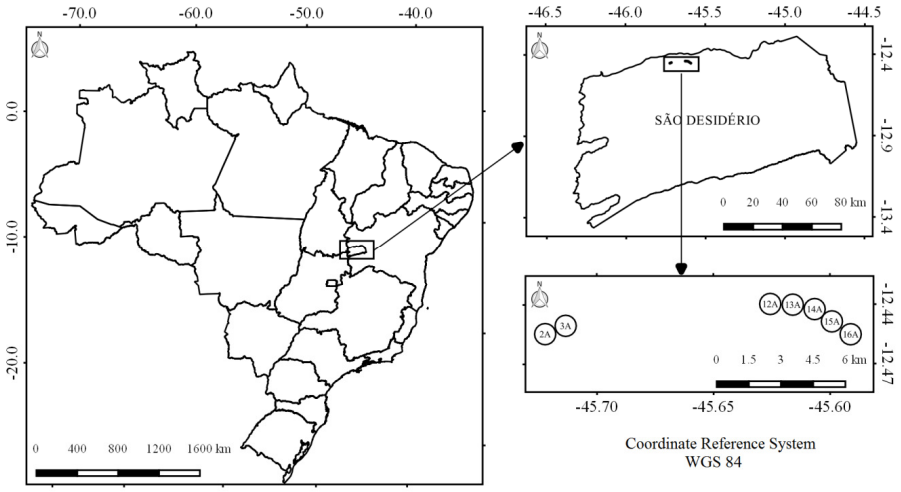

Figure 1. Map of the region of study, location in relation to the municipality of São Desidério and Brazil.

Data used referred to seven center pivots 2015's maize harvest. Each pivot (Figure 1) has a specific denomination due to the management adopted by the farm for towable pivots. For better understanding the study's methodology, a flowchart synthesizing the procedures of data acquisition and processing is presented in Figure 2.

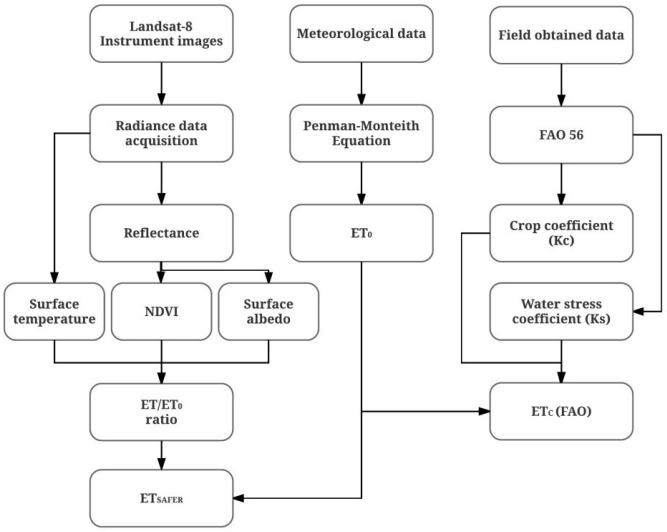

Figure 2. Data acquisition and procedures realized in order to obtain the current crop evapotranspiration through FAO-56 methodology (ETc-FAO) and SAFER algorithm (ET_{SAFER}).

Standard evapotranspiration

The meteorological data were obtained by the farm's automatic meteorological station installed within the property. The data collected were temperature, relative air humidity, solar radiation and wind speed. The estimation of reference evapotranspiration (ET_0) by the Penman-Monteith method FAO-56 (Equation 1) is according to (ALLEN et al., 1998):

$$ET_0 = \frac{0.408\Delta(Rn - G) + \gamma \frac{900}{T+273} u_2 (e_s - e_a)}{\Delta + \gamma(1 + 0.34 u_2)} \quad (1)$$

in which: ET_0 = reference evapotranspiration, mm d^{-1}; Rn = crop surface radiation balance, MJ m^{-2} d^{-1}; G = soil heat flux density, MJ m^{-2} d^{-1}; T = air temperature at 2 m above ground, °C; u_2 = wind speed at 2 m above ground, m s^{-1}; e_s = saturation vapor pressure, kPa; e_a = actual vapor pressure, kPa; Δ = slope vapor pressure curve, kPa $°C^{-1}$; and γ = psychrometric constant, kPa $°C^{-1}$.

Based on the planting and harvest dates for maize crop, the duration of each crop development phase and the Kc corresponding to each day of the cycle were estimated according to (ALLEN et al., 1998). The water stress coefficient (Ks) in which it promotes the adjustment of crop evapotranspiration as a function of the interval from one irrigation to another, meaning the current soil moisture level throughout the crop cycle was estimated according to (MANTOVANI; BERNARDO; SOARES, 2006). Thus, the deficit irrigation was obtained based on crop evapotranspiration (ETr), through Equation 2.

$$ETr = ET_0 \times Kc \times Ks \quad (2)$$

where: ETr = crop evapotranspiration, mm d^{-1}; Kc = crop coefficient, unitless; and Ks = water stress coefficient, unitless.

Simple Algorithm for Evapotranspiration Retrieving

The images related to the area were obtained through the Operational Land Imager (OLI) and Thermal Infrared Sensor (TIRS) instruments on board of the Landsat-8 satellite. The date of acquisition corresponds to the period between the planting until the end of the crop cycle. The images are provided free of charge by Land Processes Distributed Active Archive Center on the platform Earth Explorer platform, presenting a spatial resolution of 30 meters and temporal resolution of 16 days. The data were pre-analyzed and selected those that did not present cloud cover incidence, which could make unfeasible the estimation of evapotranspiration.

Before the estimation of the evapotranspiration through the SAFER algorithm, the images were previously processed with radiometric conversion and DOS1 atmospheric corrections (CHAVEZ, 1996).

The radiometric conversion consists in converting the pixels' digital numbers (DN) into physical values of radiance and reflectance, the process was performed through Equation 3.

$$L_\lambda = M_L Q_{cal} + A_L \quad (3)$$

in which: L_λ = top of atmosphere radiance, W m^{-2} $srad^{-1}$ μm^{-1}; M_L = band-specific multiplicative rescaling factor from the metadata (gain); A_L = band-specific additive rescaling factor from the metadata (offset); Q_{cal} = quantized and calibrated standard product pixel values (DN). The gain e offset values are provided in the image metadata file.

The conversion from radiance to reflectance (ρ_λ) of the OLI instrument images (bands 1 to 7) was performed according to Equation 4 (ALLEN et al., 2002; TEIXEIRA et al., 2015).

$$\rho_\lambda = \frac{\pi L_\lambda d^2}{ESUN_\lambda \cos Z} \quad (4)$$

where: ρ_λ = top of atmosphere reflectance, unitless, W m^{-2} $srad^{-1}$ μm^{-1}; $ESUN_\lambda$ = mean solar exo-atmospheric irradiances corresponding to each band of the OLI instrument, W m^{-2} sr^{-1} μm^{-1}; Z = solar zenith angle (rad); and d = Earth-sun distance in astronomical units.

To obtain evapotranspiration parameters such as planetary albedo on top of atmosphere (Equation 5), at-satellite brightness temperature (Equation 7), the methodological procedure of (TEIXEIRA et al., 2017) was adopted.

$$\alpha_{top} = \Sigma(\omega_\lambda \rho_\lambda) \quad (5)$$

in which: α_{top} = broadband planetary albedo, unitless; and ω_λ = ratio of the amount of the incoming shortwave radiation from the sun at the top of the atmosphere in a particular band and the sum for all the bands. The ω_λ was obtained through Equation 6:

$$\omega_\lambda = \frac{ESUN_\lambda}{\Sigma ESUN_\lambda} \quad (6)$$

where: $\sum ESUN\lambda_i$ = sum of all bands incoming shortwave radiation from the sun at top of atmosphere, W m^{-2} μm^{-1}.

The spectral radiance from band 10 was converted into radiometric temperatures applicable at top of atmosphere (T_{bri}) by inversion of the Planck's law in the 10.6 to 11.19 μm bandwidth.

$$T_{bri} = \frac{K2}{Ln\left(\frac{K1}{L_\lambda} + 1\right)} \quad (7)$$

in which: T_{bri} = at-satellite brightness temperature, K; K1 = band-specific thermal conversion constant, W m^{-2} μm^{-1}; and K2 = band-specific thermal conversion Constant, (K). The band-specific thermal conversion constants can be found in the image metadata file.

The α_{top} and T_{bri} values were corrected atmospherically to obtain instantaneous values of surface albedo (α_0) and temperature (T_0) using regression equations from (TEIXEIRA et al., 2009), as seen in Equations 8 and 9.

$$\alpha_0 = 0.61\ \alpha_{top} + 0.08 \quad (8)$$

$$T_0 = 1.07 T_{bri} - 20.17 \quad (9)$$

The NDVI (ROUSE et al., 1974) was obtained using the reflectance products through Equation 10.

$$NDVI = \frac{\rho_{B5} - \rho_{B4}}{\rho_{B5} + \rho_{B4}} \quad (10)$$

where: ρ_{B5} = reflectance over the wavelength ranges in near-infrared region of the solar spectrum; and ρ_{B4} = reflectance over the wavelength ranges in red region of the solar spectrum. The reflectances listed above for the Landsat-8 satellites are from bands 5 and 4, respectively.

The SAFER algorithm was then employed to model the actual and reference evapotranspiration ratio (R = ETa/ET_0) at the time the satellite overpasses the area (Equation 11):

$$R = \exp\left[\alpha + \beta\left(\frac{T_0}{\alpha_0 NDVI}\right)\right] \quad (11)$$

where, to apply the SAFER for Savanna regions, the coefficients adopted for α and β were 1.8 and -0.008 °C^{-1}, respectively, as suggested by (TEIXEIRA et al., 2013a) for semi-arid conditions.

The actual evapotranspiration is independent of crop information; therefore, a unified coefficient (K_{SAFER}), representing the interaction between Kc and Ks, may be derived by the method, a value equal to the ETa/ET_0 ratio.

ET_0, data obtained through Eq. 1 were then multiplied by the image obtained as a result from Eq. 11, resulting in the SAFER daily real evapotranspiration (ET_{SAFER}), as shown by Equation 12:

$$ET_{SAFER} = R\ ET_0 \quad (12)$$

where: ET_{SAFER}, real evapotranspiration obtained by SAFER algorithm, mm d^{-1}.

Statistical analysis

The statistical parameter indicator as a confidence or performance index (c) used to compare the values estimated by the SAFER algorithm and the values estimated by the standard method was proposed by (CAMARGO; SENTELHAS, 1997). The intervals of application validity of the models are characterized in Table 1:

Table 1. Confidence ranges of the model.

c values	Application of the model
c > 0.85	Great
0.76 ≤ c ≥ 0.85	Very good
0.66 ≤ c ≥ 0.75	Good
0.61 ≤ c ≥ 0.65	Median
0.51 ≤ c ≥ 0.60	Tolerable
0.41 ≤ c ≥ 0.50	Bad
c ≤ 0.40	Terrible

To obtain the confidence index (c) the methodology according to (CAMARGO; SENTELHAS, 1997) was used (Equation 13):

$$c = r\ d \quad (13)$$

in which: c is the coefficient of confidence or performance, unitless; r = Pearson correlation coefficient, unitless; and d is the (WILLMOTT, 1981) concordance index, unitless.

Pearson correlation coefficient and Willmott's concordance index were obtained through Equations 14 and 15.

$$r = \frac{\sum_{i=1}^{n}(O_i - \bar{O})(E_i - \bar{E})}{\sqrt{\sum_{i=1}^{n}(O_i - \bar{O})^2}.\sqrt{\sum_{i=1}^{n}(E_i - \bar{E})^2}} \quad (14)$$

$$d = 1 - \left[\frac{\sum_{i=1}^{n}(E_i - O_i)^2}{\sum_{i=1}^{n}(|E_i - \bar{O}| + |O_i - \bar{O}|)^2}\right] \quad (15)$$

where: Oi = estimated values by standard method (ETc FAO), mm d^{-1}; Ei = estimated values by SAFER (ET_{SAFER}), mm d^{-1}; and O = average estimated value by standard method (ETc FAO), mm d^{-1}.

The concordance index is a statistic that reflects the degree to which the observed variable is precisely estimated by the simulated variable. It ranges from 0 to 1, where 1 represents perfect agreement (WILLMOTT, 1981).

Also evaluated in order to verify the SAFER adjustment were the determination coefficient (r^2), mean absolute error (MAE), root mean square error (RMSE) and mean square error (MSE), as described by Equations 16 to 19.

$$r^2 = \left(\frac{\sum_{i=1}^{n}(O_i - \bar{O})(E_i - \bar{E})}{\sqrt{\sum_{i=1}^{n}(O_i - \bar{O})^2}.\sqrt{\sum_{i=1}^{n}(E_i - \bar{E})^2}}\right)^2 \quad (16)$$

$$MAE = \sum_{i=1}^{n}|E_i - O_i| \quad (17)$$

$$MSE = \frac{1}{n}\sum_{i=1}^{n}(E_i - O_i)^2 \quad (18)$$

$$RMSE = \sqrt{\frac{1}{n}\sum_{i=1}^{n}(E_i - O_i)^2} \quad (19)$$

RESULTS AND DISCUSSION

In Table 2 is presented the planting and harvesting dates of each of the studied pivots, which characterizes the period in which the observations of the Landsat-8 satellite were evaluated.

Table 2. Planting and harvesting dates of pivots under study.

Pivots	Planting date	Harvesting date	Cycle length (days)
2A	04/18/2015	08/08/2015	113
3A	04/13/2015	08/03/2015	113
12A	05/09/2015	09/24/2015	139
13A	05/12/2015	09/24/2015	136
14A	05/13/2015	09/24/2015	135
15A	05/15/2015	09/24/2015	133
16A	05/16/2015	09/24/2015	132

The different images acquired during the maize crop cycle are able to demonstrate the spatial and temporal distribution of the evapotranspiration calculated by the SAFER algorithm (Figure 3), which is a great advantage of the method for irrigation management.

The spatial variation is inherent not only by the soil type, rain spatial variation and efficiency of the irrigation system, but also by the dynamics of the irrigated area according to the development during different stages of the crop cycle. The maximum evapotranspiration estimated by SAFER is 5.38 mm d^{-1}, which is reasonable, taking in consideration that the crop was in its reproductive stage, presenting high water demand. (SOUZA; LIMA; CARVALHO, 2012), aiming to determine the evapotranspiration and maize crop coefficient, observed similar results found in this study, in which the maximum evapotranspiration of maize crop was presented during the phases corresponding to greater vegetative development, decreasing until the phase of physiological maturation.

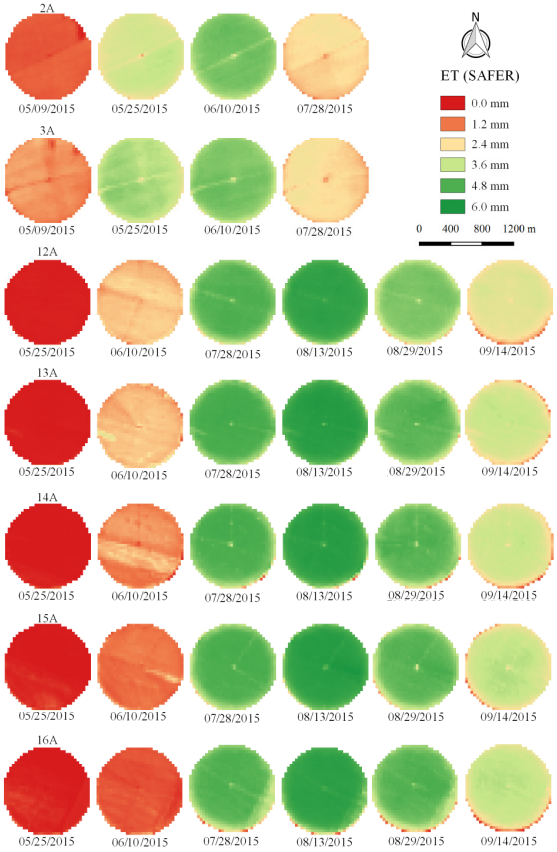

Figure 3. Spatial and temporal distribution of daily ET_{SAFER} on center pivots.

The values estimated by the standard method for crop evapotranspiration (ETc) and evapotranspiration provided by SAFER (ET_{SAFER}) are compared in Figure 4.

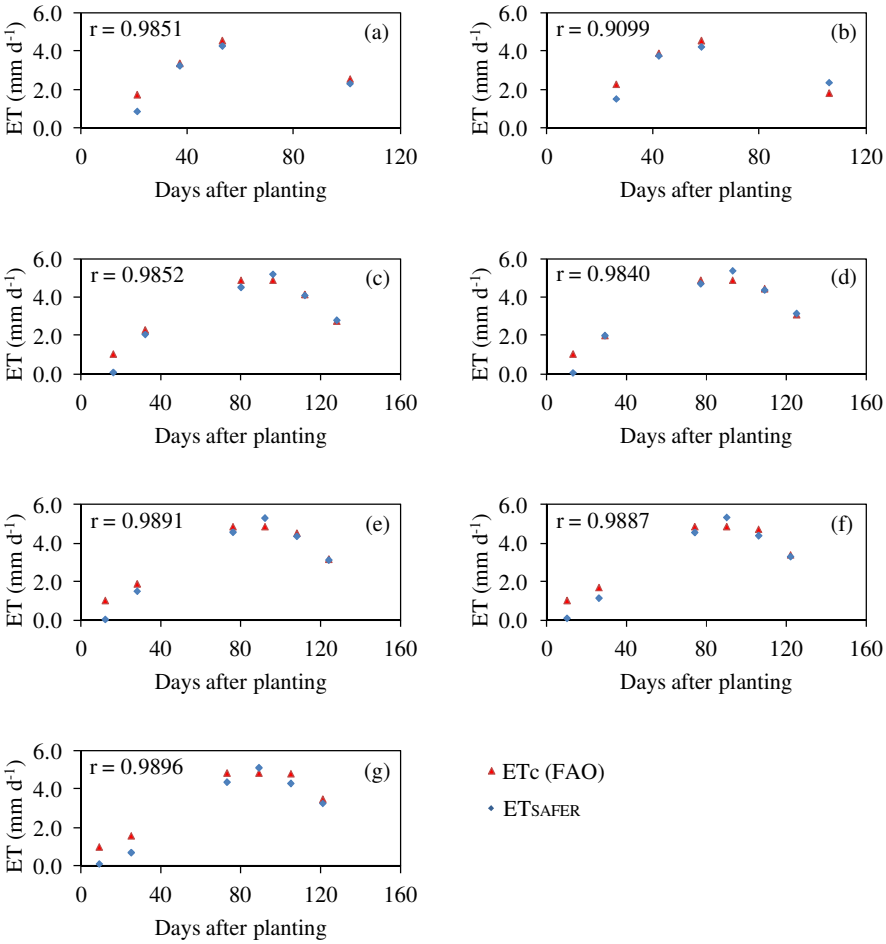

Figure 4. Comparison between ETc and ET_{SAFER} at different dates of the maize cycle for the pivots: (a) 2A; (b) 3 A; (c) 12 A; (d) 13A; (e) 14A; (f) 15A; (g) 16A.

Regarding the FAO-56 method, the SAFER showed an absolute mean error (MAE) of 0.40 mm d^{-1}. The relative error in the estimation of ET_{SAFER} using spectral images is greater when the vegetation cover is incomplete (LIU et al., 2010), as observed in the early stages of the crop cycle, up to 30 days after planting, when the SAFER algorithm method obtained smaller evapotranspiration values when compared to the standard method, reaching a maximum value of 0.99 mm d^{-1}.

The reflectance, albedo and surface temperature values obtained per pixel in the initial phase of the cycle are very different from the actual values of the crop, this is attributable to the fact that images obtained from Landsat-8 have spatial resolution of 30 m, where the average value of the pixel suffers great influence of the uncovered surface of the soil (JENSEN, 2009). According to (WARREN, 2013), the large dispersion of values also depends on the coincidence between the imaging days and the presence of irrigation in the first month and a half of the planting.

In Table 3 are presented the statistical parameters used to assess the ET_{SAFER} estimates in relation to the standard method to calculate ETr for maize crop.

Table 3. Statistical parameters of the ET_{SAFER} performance assessment in relation to ETc FAO.

r	r^2	MAE	MSE	RMSE	d	c
0.9799	0.9603	0.40	0.25	0.50	0.9749	0.9553

According to the criteria adopted by (CAMARGO; SENTELHAS, 1997), the performance index is considered great (c > 0.85). The concordance index is also considered optimal.

The magnitude of the observed errors is low, confirming the high values for Pearson's correlation coefficient and determination coefficient.

The provided actual evapotranspiration and reference evapotranspiration ratio (R) may be used as a tool to help irrigation management for different crops (TEIXEIRA, 2012), as well as monitoring the crop development. R allows values of a unified coefficient (K_{SAFER}) to be derived by the SAFER algorithm. This can be observed for the different maize cycles under this study (Figure 5), where K_{SAFER} showed sensitivity to crop development throughout its cycle.

The regression among values estimated by the standard method and SAFER algorithm are shown in Figure 6.

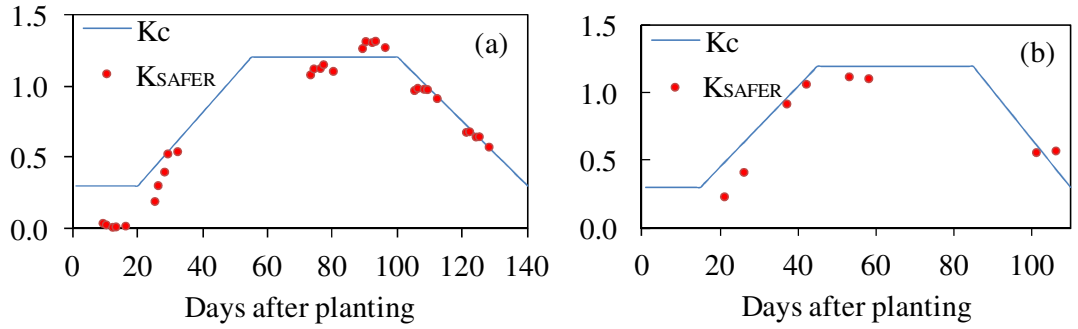

Figure 5. Kc values derived by SAFER along the cycles of maize for pivots: (a) 2A and 3A; (b) 12A, 13A, 14A, 15A and 16A.

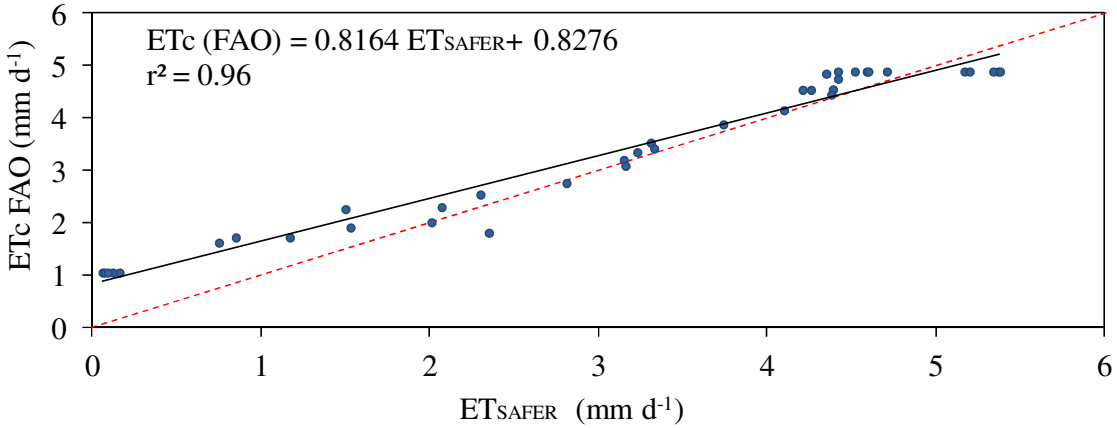

Figure 6. Comparative ETc and ET_{SAFER} for all data obtained from maize culture of the pivots under study.

The intercept coefficient parameter of the regression equation deviates from the origin due to the underestimation of the evapotranspiration values in the initial phase of the cycle, as previously discussed. The angular coefficient (multiplicative factor) is as expected, close to 1.

The SAFER algorithm presents advantages over other methods, since its estimation of evapotranspiration is a simple method that dispenses the need for specific knowledge of the radiation's physics. However, in order to become applicable to other ecosystems, there is a need for adjustments in the parameters of the equation in which the ratio of current and reference evapotranspiration is related (TEIXEIRA et al., 2013b).

Overall the SAFER algorithm showed great performance estimating the real evapotranspiration. On the contrary of the standard method, the algorithm provides the notion of evapotranspiration spatial variability, a powerful tool for irrigation management.

CONCLUSIONS

The SAFER algorithm presented estimates of the actual evapotranspiration compatible to the standard method proposed by ALLEN et al.

As advantage, the SAFER offers a greater understanding of water demand's spatial variation, thus it may be used as a tool to assist in water balance and irrigation management.

Even though precision irrigation is not a current reality, techniques similar to the SAFER algorithm may raise the perception of the variability of water requirement under an irrigation system.

RESUMO: Reconhecendo a importância da evapotranspiração como fator mediador para uma gestão de irrigação eficiente e o balanço hídrico, o objetivo desse estudo foi comparar o Simple Algorithm for Evapotranspiration Retrieving (SAFER) ao método padrão proposto no FAO-56 para estimativa de evapotranspiração real, bem como apontar sua utilidade como ferramenta de gestão de irrigação para o Cerrado brasileiro. Utilizaram-se dados referentes à safra de 2015 de sete pivôs centrais localizados no município de São Desidério, no oeste da Bahia. Para utilizar algoritmo SAFER, adotaram-se imagens adquiridas pelo satélite Landsat-8 durante o ciclo da cultura do milho. As estimativas pelo algoritmo SAFER demonstraram a variabilidade espaço-temporal da evapotranspiração. A evapotranspiração máxima de 5,38 mm d^{-1} foi observada durante o estágio reprodutivo da cultura. Em relação ao método padrão, o SAFER apresentou erro médio absoluto de 0,40 mm. Dessa forma, conclui-se que o algoritmo pode ser adotado para se estimar evapotranspiração atual da cultura como alternativa ao método padrão proposto no FAO-56 na gestão de recursos hídricos.

PALAVRAS-CHAVE: Índice de vegetação. Monitoramento da cultura. Gestão de irrigação. Balanço hídrico. Irrigação de precisão.

REFERENCES

ALLEN, R. G.; MASAHIRO, T.; MORSE, A.; TREZZA, R.; WRIGHT, J. L.; BASTIAANSSEN, W.; WILLIAM, K.; IGNACIO, L.; ROBISON, C. W. Satellite-Based Energy Balance for Mapping Evapotranspiration with Internalized Calibration (METRIC)—Applications. **Journal of Irrigation and Drainage Engineering**, v. 133, n. 4, p. 395–406, 1 ago. 2007. https://doi.org/10.1061/(asce)0733-9437(2007)133:4(395)

ALLEN, R. G.; PEREIRA, L. S.; RAES, D.; SMITH, M. **Crop evapotranspiration - Guidelines for computing crop water requirements - FAO Irrigation and drainage paper 56**. 9. ed. Food and Agriculture Organization of the United Nations, Rome: [s.n.].

ALLEN, R. G.; TASUMI, M.; TREZZA, R.; WATERS, R.; BASTIAANSSEN, W. **Surface Energy Balance Algorithms for Land: Advanced Training and Users Manual**. Idaho: Idaho Implementation, 2002. v. 1.0

ANDRADE, R.; TEIXEIRA, A. H. DE C.; SANO, E.; LEIVAS, J. F.; VICTORIA, D. C.; NOGUEIRA, S. **Evapotranspiração em Pastagens com Indicativos de Degradação na Bacia Hidrográfica do Alto Tocantins**. 1 abr. 2014. https://doi.org/10.12702/ii.inovagri.2014-a410

BASTIAANSSEN, W. G. M.; MENENTI, M.; FEDDES, R. A.; HOLTSLAG, A. A. M. A remote sensing surface energy balance algorithm for land (SEBAL). 1. Formulation. **Journal of Hydrology**, v. 212, n. Supplement C, p. 198–212, 1 dez. 1998. https://doi.org/10.1016/s0022-1694(98)00253-4

CAMARGO, A. P.; SENTELHAS, P. Avaliação do desempenho de diferentes métodos de estimativa da evapotranspiração potencial no Estado de São Paulo, Brasil. **Revista Brasileira de Agrometeorologia**, v. 5, p. 89–97, 1 jan. 1997. https://doi.org/10.13083/1414-3984.v20n02a08

CHAVEZ, P. S. Image-Based Atmospheric Corrections: Revisited and Improved. **Photogrammetric Engineering and Remote Sensing**, v. 62, n. 9, p. 1025–1036, 1996.

JENSEN, J. R. **Sensoriamento remoto do ambiente: uma perspectiva em recursos terrestres**. [s.l.] Parêntese Editora, 2009.

LIU, R.; WEN, J.; WANG, X.; WANG, L.; TIAN, H.; ZHANG, T. T.; SHI, X. K.; ZHANG, J. H.; LV, S. H. Actual daily evapotranspiration estimated from MERIS and AATSR data over the Chinese Loess Plateau. **Hydrology and Earth System Sciences**, v. 14, n. 1, p. 47–58, 2010. https://doi.org/10.5194/hess-14-47-2010

MANETA, M. P.; TORRES, M.; WALLENDER, W. W.; VOSTI, S.; KIRBY, M.; BASSOI, L. H.; RODRIGUES, L. N. Water demand and flows in the São Francisco River Basin (Brazil) with increased irrigation. **Agricultural Water Management**, v. 96, n. 8, p. 1191–1200, 1 ago. 2009. https://doi.org/10.1016/j.agwat.2009.03.008

MANTOVANI, E. M.; BERNARDO, S.; SOARES, A. A. **Manual de irrigação**. [s.l.] UFV, 2006.

RIBEIRO, J. F.; WALTER, B. M. T. Fitofisionomias do bioma Cerrado. In: **SANO, S. M.; ALMEIDA, S. P. de (Ed.). Cerrado: ambiente e flora**. Planaltina: Embrapa-CPAC, 1998. p. 87–167.

ROUSE, J. W.; HAAS, R. H.; SCHELL, J. A.; DEERING, D. W. Monitoring vegetation systems in the Great Plains with ERTS. 1974.

SANTOS, T. V.; FONTANA, D. C.; ALVES, R. C. M. Avaliação de fluxos de calor e evapotranspiração pelo modelo SEBAL com uso de dados do sensor ASTER. **Pesquisa Agropecuária Brasileira**, v. 45, n. 5, p. 488–496, 2011. https://doi.org/10.1590/s0100-204x2010000500008

SOUZA, A. P.; LIMA, M. E.; CARVALHO, D. F. Evapotranspiração e coeficientes de cultura do milho em monocultivo e em consórcio com a mucuna-cinza, usando lisímetros de pesagem. **Revista Brasileira de Ciências Agrárias**, v. 7, n. 1, p. 142–149, 2012. https://doi.org/10.5039/agraria.v7i1a802

TEIXEIRA, A. H. DE C. Modelling evapotranspiration by remote sensing parameters and agro-meteorological stations. **Remote Sensing and Hydrology (ed. by CMU Neale & MH Cosh)**, p. 154–157, 2012.

TEIXEIRA, A. H. DE C.; BASTIAANSSEN, W. G. M.; AHMAD, M. D.; BOS, M. G. Reviewing SEBAL input parameters for assessing evapotranspiration and water productivity for the Low-Middle São Francisco River basin, Brazil: Part A: Calibration and validation. **Agricultural and Forest Meteorology**, v. 149, n. 3, p. 462–476, 11 mar. 2009. https://doi.org/10.1016/j.agrformet.2008.09.016

TEIXEIRA, A. H. DE C.; HERNANDEZ, F. B. T.; LOPES, H. L.; SCHERER-WARREN, M.; BASSOI, L. H. Modelagem espaçotemporal dos componentes dos balanços de energia e de água no Semiárido brasileiro. **Embrapa Semiárido-Documentos (INFOTECA-E)**, p. 32, 2013a.

TEIXEIRA, A. H. DE C.; LEIVAS, J. F.; ANDRADE, R. G.; HERNANDEZ, F. B. T. Water productivity assessments with Landsat 8 images in the Nilo Coelho irrigation scheme. **IRRIGA**, v. 1, n. 2, p. 01, 31 ago. 2015. https://doi.org/10.15809/irriga.2015v1n2p01

TEIXEIRA, A. H. DE C.; LEIVAS, J. F.; HERNANDEZ, F. B. T.; FRANCO, R. A. M. Large-scale radiation and energy balances with Landsat 8 images and agrometeorological data in the Brazilian semiarid region. **Journal of Applied Remote Sensing**, v. 11, n. 1, p. 016030, fev. 2017. https://doi.org/10.1117/1.jrs.11.016030

TEIXEIRA, A. H. DE C.; SCHERER-WARREN, M.; HERNANDEZ, F. B.; ANDRADE, R. G.; LEIVAS, J. F. Large-scale water productivity assessments with MODIS images in a changing semi-arid environment: a Brazilian case study. **Remote Sensing**, v. 5, n. 11, p. 5783–5804, 2013b. https://doi.org/10.3390/rs5115783

THE ECONOMIST. **Brazilian Agriculture: The miracle of the cerrado**. Disponível em: <http://www.economist.com/node/16886442>. Acesso em: 11 nov. 2017.

WARREN, M. S. Desagregação espacial de estimativas de evapotranspiração real obtidas a partir do sensor MODIS. **Revista Brasileira de Meteorologia**, v. 28, n. 2, p. 153–162, jun. 2013. https://doi.org/10.1590/s0102-77862013000200004

WILLMOTT, C. J. On the Validation of Models. **Physical Geography**, v. 2, n. 2, p. 184–194, 1 jul. 1981.